Adaptive Differential Detection Using Linear Prediction for M-ary DPSK

Fumiyuki Adachi, *Senior Member, IEEE*

***Abstract*— This paper proposes a novel adaptive differential detection scheme (adaptive DD), which can significantly reduce the irreducible bit-error rate (BER) of M-ary DPSK due to Doppler spread by the adaptive linear prediction of the reference signal. The predictor coefficient is adapted to changing channel conditions by using the recursive least-square (RLS) algorithm. A phase sequence estimation based on the M-state Viterbi algorithm (VA) and another based on the decision feedback algorithm (DFA) are presented. A theoretical BER analysis is presented for adaptive DD-DFA. BER performances of 2 and 4DPSK in Rayleigh fading channels are evaluated by computer simulations. When the RLS forgetting factor of $\beta = 1$ is used, simulation results show that the irreducible BER of 4DPSK can be reduced to 7.2×10^{-5} (3.9×10^{-4}) for VA (DFA) while conventional DD offers 3.9×10^{-3} when $f_D T_b$ (maximum Doppler frequency times bit duration) $= 0.01$ and average E_b/N_0 [signal energy per bit-to-additive white Gaussian noise (AWGN) power spectrum density ratio] $= 60$ dB, where most errors are produced by Doppler spread. Adaptive DD is also effective in AWGN channels—simulations show that for the case of 4DPSK, a performance gain of 1.2 (0.7) dB is achieved over conventional DD for VA (DFA) at BER $= 10^{-3}$.**

***Index Terms*— Adaptive differential detection, linear prediction, M-ary DPSK, Rayleigh fading.**

I. Introduction

M-ARY PHASE shift keying (PSK) is a bandwidth-efficient digital modulation technique and has recently attracted increased attention in mobile radio, where the available radio bandwidth is limited. Since acquiring and tracking a reference signal for coherent detection under multipath fading environments are very difficult, if not impossible, differential detection (DD) of differentially encoded PSK (DPSK) signals is preferred. However, DD uses a delayed version of the received signal as a phase reference, and, thus, in fading channels, its bit-error rate (BER) performance exhibits an error floor (referred to as the irreducible BER due to Doppler spread or random FM noise) [1]. This is because the phase difference between two successive faded signal samples separated by one symbol duration sometimes exceeds $\pm\pi/M$ radians. The irreducible BER of M-ary DPSK increases in proportion to the second power of the normalized maximum Doppler frequency $f_D T_b$ [1], [2], where f_D is the maximum Doppler frequency given by terminal traveling speed/carrier wavelength and T_b is the bit duration. For example, the theoretical irreducible BER of 16-kbps 4DPSK becomes 3.9×10^{-3} when $f_D T_b = 0.01$, which corresponds to a traveling speed of 86.4 km/h with 2-GHz carrier frequency [2]. For lower bit rate transmission, the effect of Doppler spread becomes more severe.

In this paper, we present a novel adaptive DD scheme, which can significantly reduce the irreducible BER due to Doppler spread by the use of linear predicted reference signals and phase sequence estimation. The predictor coefficient can be adapted to changing channel conditions by using the recursive least-square (RLS) algorithm [3]. A phase sequence estimation based on the Viterbi algorithm (VA) and another based on the decision feedback algorithm (DFA) are applied. Section II describes the adaptive linear prediction of the reference signal. Section III presents the theoretical BER analysis of DFA. In Section IV, BER performances of 2 and 4DPSK in Rayleigh fading and additive white Gaussian noise (AWGN) channels are evaluated by the means of computer simulations.

Manuscript received October 6, 1994; revised November 29, 1996.

The author is with the R&D Department, NTT Mobile Communications Network, Inc., Kanagawa-ken 238, Japan (e-mail: adachi@mlab.yrp.nttdocomo.co.jp).

Publisher Item Identifier S 0018-9545(98)02482-7.

II. Adaptive Linear Prediction of Reference Signal

A. Received Signal Representation

An N-symbol sequence is assumed to be transmitted and received over a multiplicative Rayleigh fading channel. Each $\log_2 M$-bit data symbol to be transmitted is mapped onto the M-level phase difference $\Delta\phi_n \in \{2m\pi/M;\ m = 0, 1, 2, \cdots, M-1\}$. The M-ary DPSK signal can be represented in complex form as

$$s(t) = \sqrt{\frac{2E_s}{T}} \sum_{n=0}^{N} p(t - nT) \exp j\phi_n \tag{1}$$

where $\phi_n = \Delta\phi_n + \phi_{n-1}$ is the carrier phase, E_s is the signal energy per symbol (sometimes we use the signal energy per bit E_b which equals $E_s/\log_2 M$), $T = (\log_2 M)T_b$ is the symbol duration, and $p(t)$ is the low-pass equivalent impulse response of the transmit filter. For detecting the first symbol, ϕ_0 is used as the phase reference. We assume perfect automatic frequency control such that there is no frequency offset between the transmitter and receiver and perfect sampling timing. The received signal is bandlimited by the receive matched filter with a low-pass equivalent impulse response $h(t) = (1/T)p(-t)$. Assuming that the fading process is almost constant over a period of several symbols so that the receiver filter does not distort the fading process (this assumption may hold if $f_D T$ is sufficiently small,

e.g., $f_D T < 0.2$), the receive filter output can be expressed as

$$r(t) = \xi(t)\tilde{s}(t) + w(t) \tag{2}$$

where $\tilde{s}(t) = s(t) \otimes h(t)$ is the receive filter response to $s(t)$ (here, $\otimes$ is the convolution operation), $\xi(t)$ is the complex Gaussian process with unity variance which represents the effect of multiplicative Rayleigh fading, and $w(t)$ is the filtered AWGN component. We assume that the overall (transmit plus receive) filter response forms an intersymbol interference (ISI)-free Nyquist filter response at the sampling instant $t = nT$ [i.e., $\tilde{s}(nT) = \sqrt{2E_s/T}\exp j\phi_n$]. The signal sample at $t = nT$ is expressed as

$$r_n = r(nT) = \sqrt{\frac{2E_s}{T}}\,\xi_n \exp j\phi_n + w_n \tag{3}$$

where $\xi_n = \xi(nT)$ and $w_n = w(nT)$ are statistically independent zero-mean complex Gaussian variables with variances of unity and $2N_0/T$, respectively, and N_0 is the single-sided AWGN power spectrum density. Note that E_s, in the Rayleigh channel, represents average signal energy per symbol.

The conditional joint pdf of $\mathbf{r} = (r_0, r_1, \cdots, r_N)$ given $\xi = (\xi_0, \xi_1, \cdots, \xi_N)$ and $\phi = (\phi_0, \phi_1, \cdots, \phi_N)$ can be represented as

$$p(\mathbf{r}|\xi, \phi) = \frac{1}{(2\pi N_0/T)^{N+1}} \cdot \exp\left[-\frac{\sum_{n=0}^{N}\left|r_n - \sqrt{2E_s/T}\xi_n \exp j\phi_n\right|^2}{2N_0/T}\right]. \tag{4}$$

Noticing that the phase difference $\Delta\phi_n$ represents the nth-transmitted symbol, maximum-likelihood detection is to decide that the phase sequence $\Delta\overline{\phi} = (\Delta\overline{\phi}_1, \Delta\overline{\phi}_2, \cdots, \Delta\overline{\phi}_N)$ was transmitted if

$$\Lambda = \sum_{n=1}^{N} |r_n - \eta_{n-1} \exp j\Delta\phi_n|^2 \tag{5}$$

is minimized when $\Delta\phi = \Delta\overline{\phi}$, where η_{n-1} is the reference signal given by

$$\eta_{n-1} = \sqrt{2E_s/T}\,\xi_n \exp j\phi_{n-1}. \tag{6}$$

Unfortunately, ξ_n and ϕ_{n-1} are parameters unknown to the receiver. Noting that η_{n-1} equals the ensemble average of r_{n-1} if the channel is a time-invariant AWGN channel (i.e., $\xi_n = 1$ always), the conventional DD replaces η_{n-1} with the delayed signal r_{n-1} and makes a symbol-by-symbol decision—the phase $\Delta\overline{\phi}_n$ is chosen if $|r_n - r_{n-1} \exp j\Delta\overline{\phi}_n|^2$ is minimum, or equivalently $\mathrm{Re}[r_n r_{n-1}^* \exp -j\Delta\overline{\phi}_n]$ is maximum. For fading environments, however, the channel is time variant i.e., $\xi_n \neq \xi_{n-1}$, and if r_{n-1} is used as η_{n-1}, the received signal suffers from random phase variations, which cause the irreducible BER due to Doppler spread which cannot be reduced simply by increasing the received signal power. We reduce this BER by adaptively linear predicting the reference signal η_{n-1}.

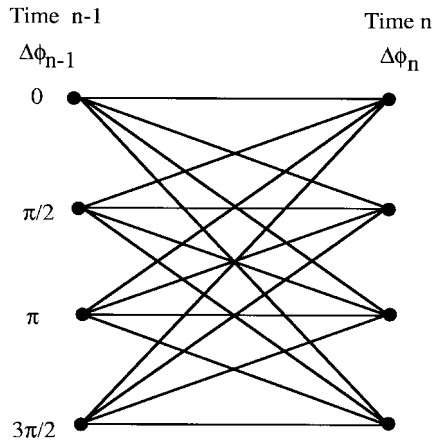

Fig. 1. Trellis diagram for 4DPSK case.

B. Linear Prediction

When fading is slow compared to the symbol rate, ξ_n can be approximated as

$$\xi_n \approx \xi_{n-1} + T\xi_{n-1}^{(1)} \tag{7}$$

where $\xi_{n-1}^{(1)}$ is the first time derivative of $\xi(t)$ at $t = (n-1)T$. Similarly, ξ_{n-1} can be approximated using ξ_{n-2} and $\xi_{n-1}^{(1)}$ as

$$\xi_{n-1} \approx \xi_{n-2} + T\xi_{n-1}^{(1)}. \tag{8}$$

From (7) and (8), a simple linear predictor of ξ_n is derived. Notice that both (7) and (8) are approximations and the effect of AWGN on prediction is ignored. We, therefore, heuristically introduce the predictor coefficient μ $(-1 \leq \mu \leq 1)$ and predict the value of ξ_n by

$$\hat{\xi}_n = \xi_{n-1} + \mu(\xi_{n-1} - \xi_{n-2}). \tag{9}$$

Replacing ξ_n in (6) with $\hat{\xi}_n$, we obtain the following reference signal prediction:

$$\hat{\eta}_{n-1} = r_{n-1} + \mu(r_{n-1} - r_{n-2} \exp j\Delta\phi_{n-1}) \tag{10}$$

which is a two-tap forward linear predictor [3] modified for DD. The predictor coefficient μ is adapted to changing channel conditions. The adaptation algorithm of μ is described in Section II-D.

C. Sequence Estimation

The phase sequence that minimizes (5) with η_{n-1} replaced by $\hat{\eta}_{n-1}$ is chosen. This sequence estimation can be performed recursively based on the M-state VA. The trellis diagram is shown, as an example for the 4DPSK case, in Fig. 1. At time n (i.e., $t = nT$), there are M phase states of $\Delta\phi_n$. The branch metric from the particular phase state of $\Delta\phi_{n-1}$ to that of $\Delta\phi_n$ is represented as

$$\lambda(\Delta\phi_{n-1} \to \Delta\phi_n) = |r_n - \hat{\eta}_{n-1}(\Delta\phi_{n-1}) \exp j\Delta\phi_n|^2 \tag{11}$$

where $\hat{\eta}_{n-1}(\Delta\phi_{n-1})$ is the linear predicted reference signal at the particular phase state of $\Delta\phi_{n-1}$ and is derived from (10).

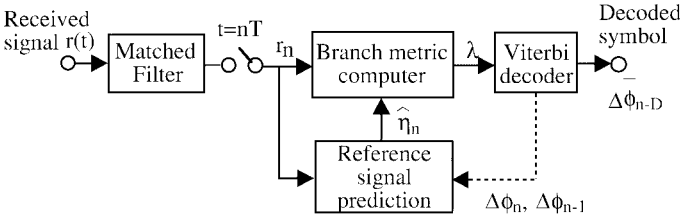

Fig. 2. Adaptive DD detector structure.

The path metric $\Lambda(\Delta\phi_n)$ is defined as

$$\Lambda(\Delta\phi_n) = \lambda(\Delta\phi_{n-1} \rightarrow \Delta\phi_n) + \Lambda(\Delta\phi_{n-1}). \tag{12}$$

M-possible paths enter into each phase state of $\Delta\phi_n$. The path having the minimum path metric is selected, and the others are discarded. Since there are M phase states at time n, a total of M paths survive. The survivor path having the minimum path metric is traced D steps back to make a decision on the $n-D$th symbol, $\Delta\phi_{n-D}$; the detected output is represented as $\Delta\overline{\phi}_{n-D}$. The block diagram of the adaptive DD receiver is illustrated in Fig. 2. The receiver is composed of the branch metric computer, Viterbi decoder, and reference signal predictor.

If only one path is allowed to survive at time n, the VA reduces to symbol-by-symbol decision based on the DFA. The branch metric given by (11) can be used as a decision variable. $\Delta\overline{\phi}_n$ is determined as the transmitted symbol if $\Delta\phi_n = \Delta\overline{\phi}_n$ minimizes the metric $\lambda(\Delta\phi_n) = |r_n - \hat{\eta}_{n-1}(\Delta\overline{\phi}_{n-1}) \exp j\Delta\phi_n|^2$. Since the value of $\hat{\eta}_{n-1}(\Delta\overline{\phi}_{n-1})$ is the same for all possible M phase states of $\Delta\phi_n$, the decision can be modified to

$$\Delta\overline{\phi}_n = \max_{\Delta\phi_n} \mathrm{Re}[r_n\hat{\eta}^*_{n-1}(\Delta\overline{\phi}_{n-1}) \exp -j\Delta\phi_n]. \tag{13}$$

D. Predictor Coefficient Adaptation Algorithm

Mobile radio channel conditions vary from time to time with the movement of the mobile terminal, e.g., from an AWGN channel to a Rayleigh channel and vice versa. In practice, therefore, it is necessary to track the variations of the channel conditions. A stochastic adaptation algorithm of the predictor coefficient based on the RLS algorithm is developed.

Denote $\mu_n(\Delta\phi_n)$ as the value of μ at the particular phase state of $\Delta\phi_n$ at time n. After determining the M survivor paths, each path leads to one of the M phase states of $\Delta\phi_n$, and the predictor coefficient is updated so that the following exponentially weighted prediction error J is minimized:

$$J = \sum_{l=0}^{n-1} \beta^l |r_{n-l} - \tilde{\eta}_{n-1-l} \exp j\Delta\phi_{n-l}|^2 \tag{14}$$

where β is the forgetting factor ($0 < \beta \leq 1$) and $\tilde{\eta}_{n-1-l}$ is the reference signal at time $n-l$, $l = 1, 2, \cdots, n-1$ that is predicted using the same predictor coefficient $\mu_n(\Delta\phi_n)$. Note that $\Delta\phi_{n-l}$, in this case, represents the phase sequence along the survivor path leading to the particular phase state of $\Delta\phi_n$. $\tilde{\eta}_{n-1-l}$ is expressed as

$$\tilde{\eta}_{n-1-l} = r_{n-1-l} + \mu_n(\Delta\phi_n) \cdot (r_{n-1-l} - r_{n-2-l} \exp j\Delta\phi_{n-1-l}). \tag{15}$$

Substituting (15) into (14), the value of $\mu_n(\Delta\phi_n)$, which minimizes J, is found to be as shown in (16), given at the bottom of the page. From (16), the following recursive adaptation algorithm of $\hat{\mu}_n$ is formulated:

$$\begin{cases} \hat{\mu}_n(\Delta\phi_n) = \dfrac{\Theta_n(\Delta\phi_n)}{\Omega_n(\Delta\phi_n)} \\ \Theta_n(\Delta\phi_n) = \beta\Theta_{n-1}(\Delta\phi_{n-1}) + \mathrm{Re}[(r_n - r_{n-1} \exp j\Delta\phi_n) \cdot (r_{n-1} - r_{n-2} \exp j\Delta\phi_{n-1})^* \exp -j\Delta\phi_n] \\ \Omega_n(\Delta\phi_n) = \beta\Omega_{n-1}(\Delta\phi_{n-1}) + |r_{n-1} - r_{n-2} \exp j\Delta\phi_{n-1}|^2 \\ \Theta_0 = 0,\ \Omega_0 = \delta \text{ (small positive value)},\ r_{-1} = 0 \\ \Delta\phi_0 = 0, \qquad 0 < \beta \leq 1. \end{cases} \tag{17}$$

E. Convergence of Predictor Coefficient

The convergence of the predictor coefficient in two special channel cases is considered: AWGN and Rayleigh channels. Since the received signal sample sequence is a stationary process, the values of Θ_n and Ω_n approach the ensemble averages of $(1-\beta)^{-1}\mathrm{Re}[(r_n - r_{n-1} \exp j\Delta\phi_n)(r_{n-1} - r_{n-2} \exp j\Delta\phi_{n-1})^* \exp -j\Delta\phi_n]$ and $(1-\beta)^{-1}|r_{n-1} - r_{n-2} \exp j\Delta\phi_{n-1}|^2$, respectively, as time elapses. We assume here no decision errors have been made. The ensemble averages $E(\Theta_n)$ and $E(\Omega_n)$ can be obtained as

$$\begin{cases} E(\Theta_n) = -\dfrac{1}{1-\beta} \dfrac{2N_0}{T} \left[\dfrac{E_s}{N_0} \{1 - \mathrm{Re}[2\rho(T) - \rho(2T)]\} + 1 \right] \\ E(\Omega_n) = \dfrac{1}{1-\beta} \dfrac{4N_0}{T} \left[\dfrac{E_s}{N_0} \{1 - \mathrm{Re}[\rho(T)]\} + 1 \right] \end{cases} \tag{18}$$

where $\rho(kT)$ is the autocorrelation function of ξ_n defined by

$$\rho(kT) = \frac{E(\xi_n \xi^*_{n-k})}{E(|\xi_n|^2)}. \tag{19}$$

Thus, the predictor coefficient may converge to

$$\mu_\infty = -\frac{1}{2} \frac{1 + \dfrac{E_s}{N_0}\{1 - \mathrm{Re}[2\rho(T) - \rho(2T)]\}}{1 + \dfrac{E_s}{N_0}\{1 - \mathrm{Re}[\rho(T)]\}}. \tag{20}$$

The value of μ_∞ depends on the maximum Doppler frequency f_D and the signal energy per symbol-to-AWGN power spectrum density ratio E_s/N_0. For small $f_\mathrm{D}T$ values, $\rho(kT)$ can be

$$\hat{\mu}_n(\Delta\phi_n) = \frac{\mathrm{Re}\left[\sum_{l=0}^{n-1} \beta^l (r_{n-l} - r_{n-1-l} \exp j\Delta\phi_{n-l})(r_{n-1-l} - r_{n-2-l} \exp j\Delta\phi_{n-1-l})^* \exp -j\Delta\phi_{n-l}\right]}{\sum_{l=0}^{n-1} \beta^l |r_{n-1-l} - r_{n-2-l} \exp j\Delta\phi_{n-1-l}|^2} \tag{16}$$

approximated as $\rho(kT) \approx 1+\rho^{(1)}(0)T+\rho^{(2)}(0)T^2/2$, where $\rho^{(m)}(0)$ is the mth-order time derivative of $\rho(t)$ at $t = 0$. Using this approximation and since $\rho^{(1)}(0)$ is imaginary, (20) becomes

$$\mu_\infty \approx -\frac{1}{2}\frac{1+\dfrac{E_s}{N_0}\rho^{(2)}(0)T^2}{1-\dfrac{E_s}{N_0}\rho^{(2)}(0)\dfrac{T^2}{2}}. \tag{21}$$

In a land mobile radio channel, $\rho(kT) = J_0(2k\pi f_{\rm D}T)$ [1], where $J_0(.)$ is the zeroth-order Bessel function of the first kind, so (21) becomes

$$\mu_\infty \approx \frac{-0.5+\dfrac{E_s}{N_0}(\pi f_{\rm D}T)^2}{1+\dfrac{E_s}{N_0}(\pi f_{\rm D}T)^2} \tag{22}$$

for small values of $f_{\rm D}T$.

For large values of E_s/N_0, decision errors are predominantly produced by fading-induced phase variations. In this case, substituting $E_s/N_0 \to \infty$ into (22), we find that μ_∞ becomes unity. On the other hand, for very slow Rayleigh channels, i.e., $f_{\rm D}T \to 0$, the AWGN is a major cause of errors as in the AWGN channel. Substituting $f_{\rm D}T = 0$ into (22) gives $\mu_\infty = -0.5$ in this case. It is interesting to note that when $\hat{\mu}_n = -0.5$ is always used, the reference signal becomes

$$\hat{\eta}_{n-1} = 0.5(r_{n-1} + r_{n-2}\exp j\Delta\phi_{n-1}) \tag{23}$$

which is identical to the reference signal of multiple-symbol DD using $L = 2$ samples [4]–[6] (note that in [4] notation λ is used instead of L). This implies that the adaptive DD can also reduce the BER in AWGN channels. For the fading case, the irreducible BER due to Doppler spread can be reduced through linear prediction of the reference signal. As a consequence, adaptive DD can reduce not only the irreducible BER due to Doppler spread, but also the BER due to AWGN by adapting the predictor coefficient to the varying channel conditions. This will be proved later theoretically and by computer simulation.

F. Summary

The proposed adaptive DD algorithms are summarized below.

1) VA:

a) Branch metric:

$$\lambda(\Delta\phi_{n-1}\to\Delta\phi_n) = |r_n - \hat{\eta}_{n-1}(\Delta\phi_{n-1})\exp j\Delta\phi_n|^2. \tag{24}$$

b) Path metric:

$$\Lambda(\Delta\phi_n) = \lambda(\Delta\phi_{n-1}\to\Delta\phi_n) + \Lambda(\Delta\phi_{n-1}). \tag{25}$$

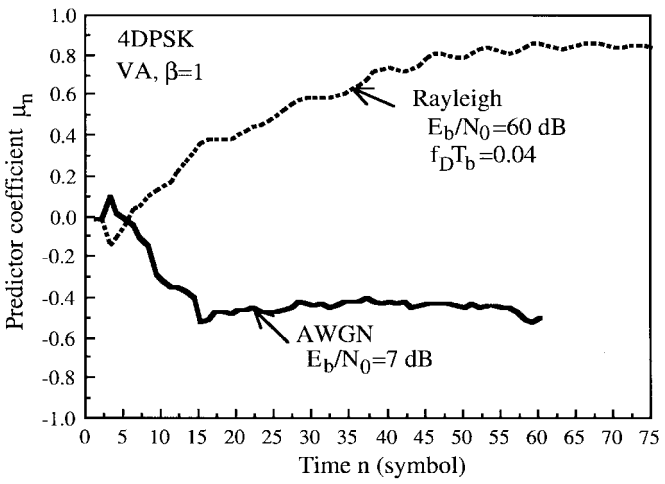

Fig. 3. Convergence of predictor coefficient.

c) Linear prediction:

$$\hat{\eta}_{n-1}(\Delta\phi_{n-1}) = r_{n-1} + \hat{\mu}_{n-1}(\Delta\phi_{n-1}) \cdot (r_{n-1} - r_{n-2}\exp j\Delta\phi_{n-1}). \tag{26}$$

d) Predictor coefficient adaption: See (27), given at the bottom of the page.

The VA traces the survivor path that has the minimum path metric at time n back D steps to make a decision on $\Delta\phi_{n-D}$. This incurs D-symbol decision delay.

2) DFA:

$$\Delta\bar{\phi}_n = \max_{\Delta\phi_n} {\rm Re}[r_n\hat{\eta}^*_{n-1}(\Delta\bar{\phi}_{n-1})\exp -j\Delta\phi_n]. \tag{28}$$

The linear prediction of the reference signal and the predictor coefficient adaptation algorithm are the same for the VA.

III. BER Analysis

A BER analysis of adaptive DD-DFA is presented here since the VA is difficult to analyze. Once a decision error is produced by noise, the reference signal is wrongly phase rotated if the incorrectly detected symbol is fedback, so the next decision will likely be in error. This succeeding error rotates back the reference signal into the correct phase, and, thus, most errors result in double symbol errors [6]. As a consequence, the average BER of adaptive DD-DFA with detected symbol feedback can be well approximated as

$$P_{\rm DFA,\,detected\,symbol} \approx 2P_{\rm DFA,\,correct\,symbol} \tag{29}$$

$$\begin{cases} \hat{\mu}_n(\Delta\phi_n) = \dfrac{\Theta_n(\Delta\phi_n)}{\Omega_n(\Delta\phi_n)} \\ \Theta_n(\Delta\phi_n) = \beta\Theta_{n-1}(\Delta\phi_{n-1}) + {\rm Re}[(r_n - r_{n-1}\exp j\Delta\phi_n) \\ \qquad \cdot(r_{n-1} - r_{n-2}\exp j\Delta\phi_{n-1})^*\exp -j\Delta\phi_n] \\ \Omega_n(\Delta\phi_n) = \beta\Omega_{n-1}(\Delta\phi_{n-1}) + |r_{n-1} - r_{n-2}\exp j\Delta\phi_{n-1}|^2 \\ \Theta_0 = 0,\ \Omega_0 = \delta \text{ (small positive value)},\ r_{-1} = 0 \\ \qquad \Delta\phi_0 = 0, \qquad 0 < \beta \le 1 \end{cases} \tag{27}$$

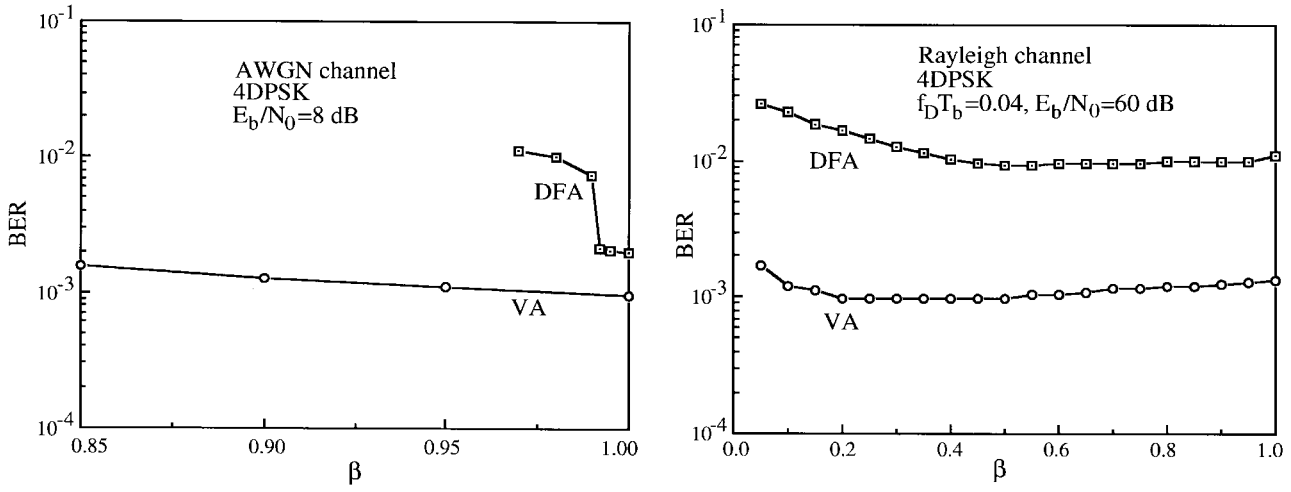

(a) (b)

Fig. 4. Effect of forgetting factor on predictor coefficient adaptation. (a) AWGN channel. (b) Rayleigh channel.

where $P_{\text{DFA, correct symbol}}$ is the BER with correct symbol feedback. From (28), $P_{\text{DFA, correct symbol}}$ is derived from the probability of the phase angle ψ between the received signal r_n and the reference signal $\hat{\eta}_{n-1}$. Equation (29) is valid only if the decision errors with correct symbol feedback are sufficiently isolated—this condition holds for small BER regions, e.g., less than about 10^{-2}. Hence, (29) cannot be applied to the case of slow fading, where errors are bursty. The approximate analysis can be applied to fading channels with large E_s/N_0 values (where errors are predominantly produced by Doppler spread) as well as AWGN channels.

A. AWGN Channel

Without loss of generality, all zero-symbol transmission is assumed, i.e., $\Delta\phi_n = 0$ for all n. Assuming correct symbol feedback, $\hat{\eta}_{n-1}$ becomes a complex Gaussian variable. Applying [7], the probability distribution of ψ is expressed as $\text{Prob}[\Psi > \psi \geq -\pi] = F(\Psi) - F(-\pi) + u(\Psi)$, where $u(z) = 1$ for $z \geq 0$ and zero otherwise and

$$F(\psi) = \frac{-W \sin\psi}{4\pi} \int_{-(\pi/2)}^{+(\pi/2)} \cdot \frac{\exp\left[-(U - V\sin t - W\cos\psi\cos t)\right]}{U - V\sin t - W\cos\psi\cos t}\, dt \quad (30)$$

with $U = 0.5(\rho_r + \rho^\eta)$, $V = 0.5(\rho_r - \rho^\eta)$, and $W = \sqrt{\rho_r\rho_\eta}$ and ρ_r and ρ_η are the signal-to-noise ratios (SNR's) of r_n and $\hat{\eta}_{n-1}$, respectively. The SNR of r_n is $\rho_r = E_s/N_0$. Since $\xi_n = \xi$ with $|\xi| = 1$ (the channel is time invariant)

$$\begin{cases} E(\hat{\eta}_{n-1}) = \sqrt{\dfrac{2E_s}{T}}\,\xi \\ \text{var}(\hat{\eta}_{n-1}) = \{(1+\hat{\mu}_{n-1})^2 + \hat{\mu}_{n-1}^2\}\,\dfrac{2N_0}{T} \end{cases} \quad (31)$$

and ρ_η becomes

$$\rho_\eta = \frac{|E(\hat{\eta}_{n-1})|^2}{\text{var}(\hat{\eta}_{n-1})} = 2\,\frac{E_s}{N_0} \quad (32)$$

when $\mu_{n-1} = -0.5$ is always used (since the value of $\hat{\mu}_n$ converges to $\mu_\infty = -0.5$ in AWGN channels). Hence, we have $U = 1.5E_s/N_0$, $V = -0.5E_s/N_0$, and $W = \sqrt{2}E_s/N_0$.

Since the phase noise distribution is symmetric around $\psi = 0$, it is sufficient to consider the negative region of ψ. We assume the Gray-code bit mapping rule. From [10], we can find the relationship between the error region and the Hamming distance. For 2DPSK, a bit error is produced when $\psi < -\pi/2$ and the BER with correct symbol feedback is given by $P_{\text{DFA, correct symbol}} = 2F(-\pi/2)$. For 4DPSK, single-bit error is produced when $-3\pi/4 \leq \psi < -\pi/4$ and two-bit error when $-\pi \leq \psi < -3\pi/4$, and thus we have $P_{\text{DFA, correct symbol}} = F(-\pi/4) + F(-3\pi/4)$. For $M \geq 8$, the BER can be approximated as $P_{\text{DFA, correct symbol}} = (2/\log_2 M)F(-\pi/M)$. Noting that the probability of ψ falling into error regions other than the nearest region $-3\pi/M \leq \psi < -\pi/M$ can be neglected for large E_s/N_0, we obtain the following BER expression that can be applied to any value of M:

$$P_{\text{DFA, correct symbol}} = \frac{a(M)}{\log_2 M}\left[F\left(-\frac{\pi}{M}\right) + F\left(-\pi + \frac{\pi}{M}\right)\right] \quad (33)$$

where $a(M) = 1$ (2) for $M = 2$ (≥ 4). Equation (33) is exact for $M = 2$ and 4 while it is an approximation for $M \geq 8$. Substituting (30) into the above and taking into account decision error propagation, the BER for DFA with *detected symbol feedback* is approximately given by

$$P_{\text{DFA, detected symbol}} \approx \frac{a(M)}{\log_2 M}\,\frac{\sqrt{2}\sin\dfrac{\pi}{M}}{\pi} \int_0^\pi \cdot \frac{\exp\left[-\dfrac{E_s}{N_0}\left(\dfrac{3}{2} - \sqrt{\dfrac{1}{4} + 2\cos^2\dfrac{\pi}{M}}\cos t\right)\right]}{\dfrac{3}{2} - \sqrt{\dfrac{1}{4} + 2\cos^2\dfrac{\pi}{M}}\cos t}\, dt. \quad (34)$$

For comparison, we consider conventional DD and coherent detection with differential decoding (hereafter, referred to as

CD). When $\hat{\mu}_n$ always equals zero, adaptive DD reduces to conventional DD. There is no error propagation, and $\rho_r = \rho_\eta = E_s/N_0$. For deriving the BER of CD, we refer to [10]. The BER expressions for the two detection schemes are given by

$$\begin{cases} P_{\text{conventional DD}} = \dfrac{a(M)}{\log_2 M}\dfrac{\sin\dfrac{\pi}{M}}{2\pi}\displaystyle\int_0^{\pi} \cdot \dfrac{\exp\left[-\dfrac{E_s}{N_0}\left(1-\cos\dfrac{\pi}{M}\cos t\right)\right]}{1-\cos\dfrac{\pi}{M}\cos t}\,dt \\ P_{\text{CD}} = \dfrac{a(M)}{\log_2 M}\operatorname{erfc}\left(\sqrt{\dfrac{E_s}{N_0}}\sin\dfrac{\pi}{M}\right)\left[1-\dfrac{1}{2}\operatorname{erfc}\left(\sqrt{\dfrac{E_s}{N_0}}\sin\dfrac{\pi}{M}\right)\right] \end{cases} \tag{35}$$

which are approximations for $M \geq 8$. In particular, when $M = 2$, we have $P_{\text{conventional DD}} = 0.5\exp[-E_s/N_0]$. The BER performances of adaptive DD-DFA, conventional DD, and CD calculated from (34) and (35) are plotted in Fig. 8 as solid lines for $M = 2$ and 4.

To see how much performance is gained by adaptive DD, we examine the asymptotic behavior (at large E_s/N_0 values) of (34). From the Appendix, we obtain

$$P_{\text{DFA, detected symbol}} \approx \frac{a(M)}{\log_2 M}\operatorname{erfc}\sqrt{\frac{1}{2}\frac{E_s}{N_0}\left(3-\sqrt{1+8\cos^2\frac{\pi}{M}}\right)} \tag{36}$$

for large E_s/N_0. We readily observe that adaptive DD-DFA approaches CD with a performance loss of 1.2 dB for 4DPSK ($M = 4$) and that for 2DPSK ($M = 2$), its BER performance is close to that of CD.

B. BER Due to Doppler Spread

In AWGN channels, the phase noise ψ is symmetrically distributed about $\psi = 0$. However, in fading, the phase noise distribution is not necessary symmetric—when the power spectrum of $\xi(t)$ is asymmetric, the phase noise distribution becomes asymmetric. Thus, we need to consider the entire range of ψ. We obtain

$$P_{\text{DFA, correct symbol}} = \frac{a(M)}{2}\frac{P_+ + P_-}{\log_2 M} \tag{37}$$

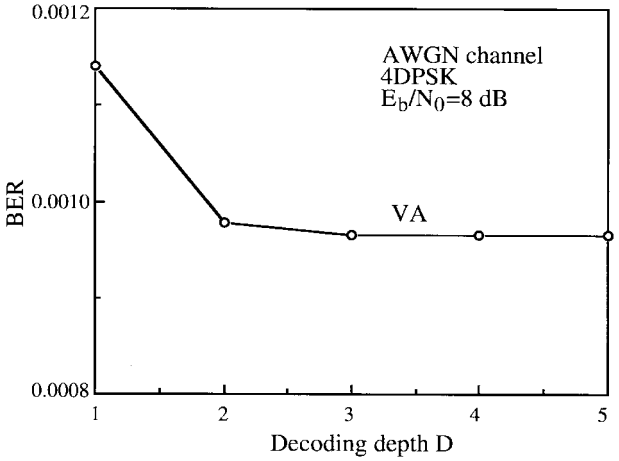

Fig. 5. Effect of decoding depth for VA.

where

$$\begin{cases} P_+ = \text{Prob}\left[-\dfrac{\pi}{M} \geq \psi \geq -\pi\right] \\ \qquad +\text{Prob}\left[\pi > \psi \geq \pi - \dfrac{\pi}{M}\right] \\ P_- = \text{Prob}\left[\pi > \psi \geq \dfrac{\pi}{M}\right] \\ \qquad +\text{Prob}\left[-\pi + \dfrac{\pi}{M} \geq \psi \geq -\pi\right]. \end{cases} \tag{38}$$

When the phase noise distribution is symmetric with respect to $\psi = 0$, (37) reduces to (33). The probability distribution of ψ in Rayleigh fading is expressed as [9]

$$\begin{aligned} &\text{Prob}[\Psi \geq \psi \geq -\pi] \\ &\quad = \frac{1}{2}\left[1+\frac{\Psi}{\pi}+\frac{2}{\pi}\frac{\sqrt{r^2+\lambda^2}\sin(\Psi-\alpha)}{\sqrt{1-(r^2+\lambda^2)\cos^2(\Psi-\alpha)}}\right. \\ &\qquad \cdot \tan^{-1}\sqrt{\frac{1+\sqrt{r^2+\lambda^2}\cos(\Psi-\alpha)}{1-\sqrt{r^2+\lambda^2}\cos(\Psi-\alpha)}} \\ &\qquad -\frac{2}{\pi}\frac{\sqrt{r^2+\lambda^2}\sin\alpha}{\sqrt{1-(r^2+\lambda^2)\cos^2\alpha}} \\ &\qquad \left.\cdot \tan^{-1}\sqrt{\frac{1-\sqrt{r^2+\lambda^2}\cos\alpha}{1+\sqrt{r^2+\lambda^2}\cos\alpha}}\right] \end{aligned} \tag{39}$$

as shown in (40), given at the bottom of the page. From (39) and using the trigonometric equation $\tan^{-1}a + \tan^{-1}(1/a) =$

$$\begin{cases} r + j\lambda = \dfrac{E(r_n\hat{\eta}^*_{n-1})}{\sqrt{E(|r_n|^2)E(|\hat{\eta}_{n-1}|^2)}} \\ \qquad = \dfrac{\dfrac{E_s}{N_0}\{(1+\hat{\mu}_{n-1}\rho(T)-\hat{\mu}_{n-1}\rho(2T)\}}{\sqrt{\dfrac{E_s}{N_0}+1}\sqrt{\dfrac{E_s}{N_0}\{(1+\hat{\mu}_{n-1})^2+\hat{\mu}^2_{n-1}-2\hat{\mu}_{n-1}(\hat{\mu}_{n-1}+1)\text{Re}[\rho(T)]\}+(1+\hat{\mu}_{n-1})^2+\hat{\mu}^2_{n-1}}} \\ \alpha = \tan^{-1}\dfrac{\lambda}{r} \end{cases} \tag{40}$$

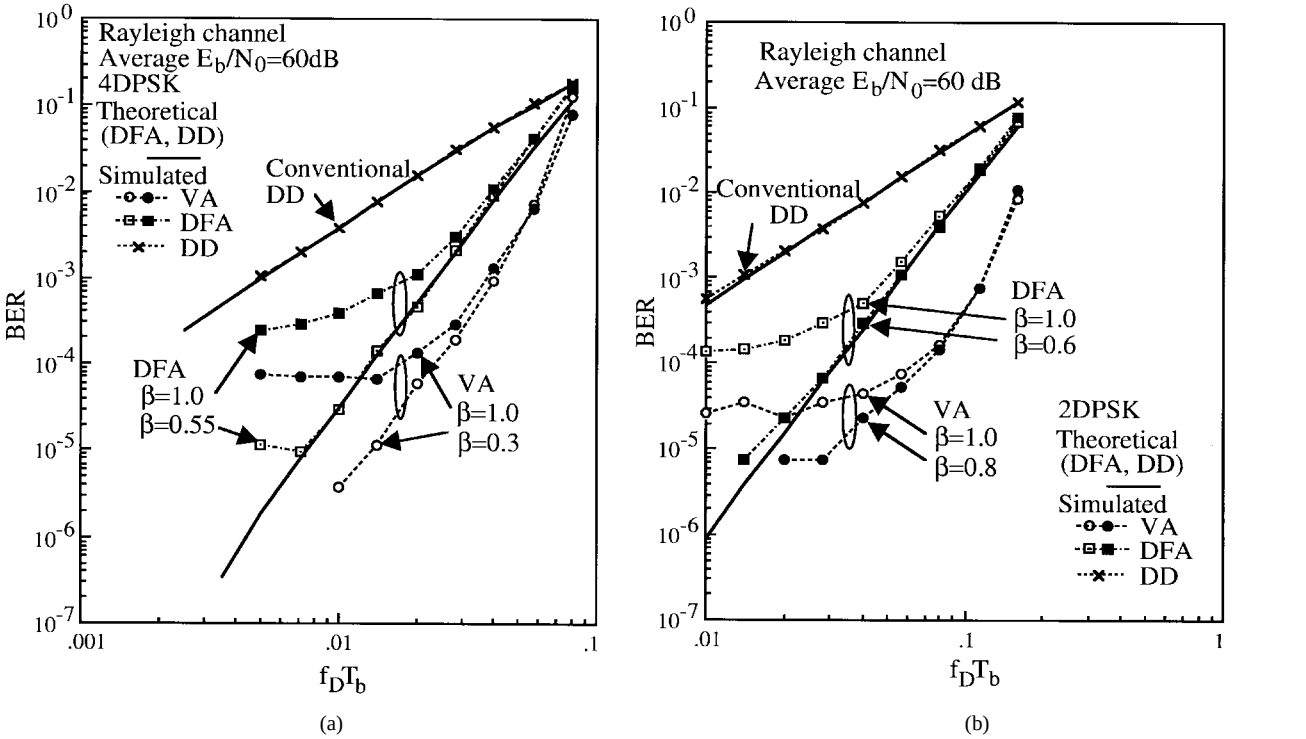

Fig. 6. Irreducible BER due to Doppler spread: (a) 4DPSK and (b) 2DPSK.

$\pi/2$, $P_{\pm}$ becomes

$$P_{\pm} = \frac{1}{2}\left[1 - \frac{\sqrt{r^2+\lambda^2}\,\sin\left(\frac{\pi}{M} \pm \alpha\right)}{\sqrt{1-(r^2+\lambda^2)\cos^2\left(\frac{\pi}{M} \pm \alpha\right)}}\right] \tag{41}$$

which is substituted into (37) to obtain $P_{\text{DFA, correct symbol}}$. When *detected symbols* are fedback, the BER becomes approximately twice the value of $P_{\text{DFA, correct symbol}}$ [see (29)] and therefore is given by

$$P_{\text{DFA, detected symbol}} = \frac{a(M)}{\log_2 M}\left\{1 - \frac{1}{2}\left[\frac{\sqrt{r^2+\lambda^2}\,\sin\left(\frac{\pi}{M}+\alpha\right)}{\sqrt{1-(r^2+\lambda^2)\cos^2\left(\frac{\pi}{M}+\alpha\right)}} + \frac{\sqrt{r^2+\lambda^2}\,\sin\left(\frac{\pi}{M}-\alpha\right)}{\sqrt{1-(r^2+\lambda^2)\cos^2\left(\frac{\pi}{M}-\alpha\right)}}\right]\right\} \tag{42}$$

which is an approximation for $M \geq 8$. Note that as discussed earlier, this approximation can be applied only to derive the irreducible BER due to Doppler spread. Letting $E_s/N_0 \to \infty$ and using $\hat{\mu}_{n-1} = 1$ (the value of $\hat{\mu}_n$ converges to $\mu_\infty = 1$ for large E_s/N_0 in Rayleigh fading) in (40), $r + j\lambda$ becomes

$$r + j\lambda = \frac{2\rho(T) - \rho(2T)}{\sqrt{5 - 4\text{Re}[\rho(T)]}}. \tag{43}$$

For comparison, we consider conventional DD. Because there is no error propagation, we do not need to restrict our analysis to the irreducible BER due to Doppler spread. Substituting $r + j\lambda$ with $\hat{\mu}_{n-1} = 0$ into (42) and dividing by two gives the exact BER expression for conventional DD

$$P_{\text{conventional DD}} = \frac{a(M)}{2\log_2 M}\left\{1 - \frac{1}{2}\left[\frac{\sqrt{r^2+\lambda^2}\,\sin\left(\frac{\pi}{M}+\alpha\right)}{\sqrt{1-(r^2+\lambda^2)\cos^2\left(\frac{\pi}{M}+\alpha\right)}} + \frac{\sqrt{r^2+\lambda^2}\,\sin\left(\frac{\pi}{M}-\alpha\right)}{\sqrt{1-(r^2+\lambda^2)\cos^2\left(\frac{\pi}{M}-\alpha\right)}}\right]\right\} \tag{44}$$

where

$$r + j\lambda = \frac{\frac{E_s}{N_0}\rho(T)}{\frac{E_s}{N_0} + 1}. \tag{45}$$

To see how much performance gain is obtained by adaptive DD against the irreducible BER due to Doppler spread, we assume $\rho(kT) = J_0(2k\pi f_D T)$ as in Section II. From (43), we have $\lambda = 0$, and, thus, $\alpha = 0$. Using the power series expansion of $J_0(2k\pi f_D T)$ with respect to $f_D T$, we have $r \approx 1 - (\pi f_D T)^4$ for adaptive DD and $1 - (\pi f_D T)^2$ for

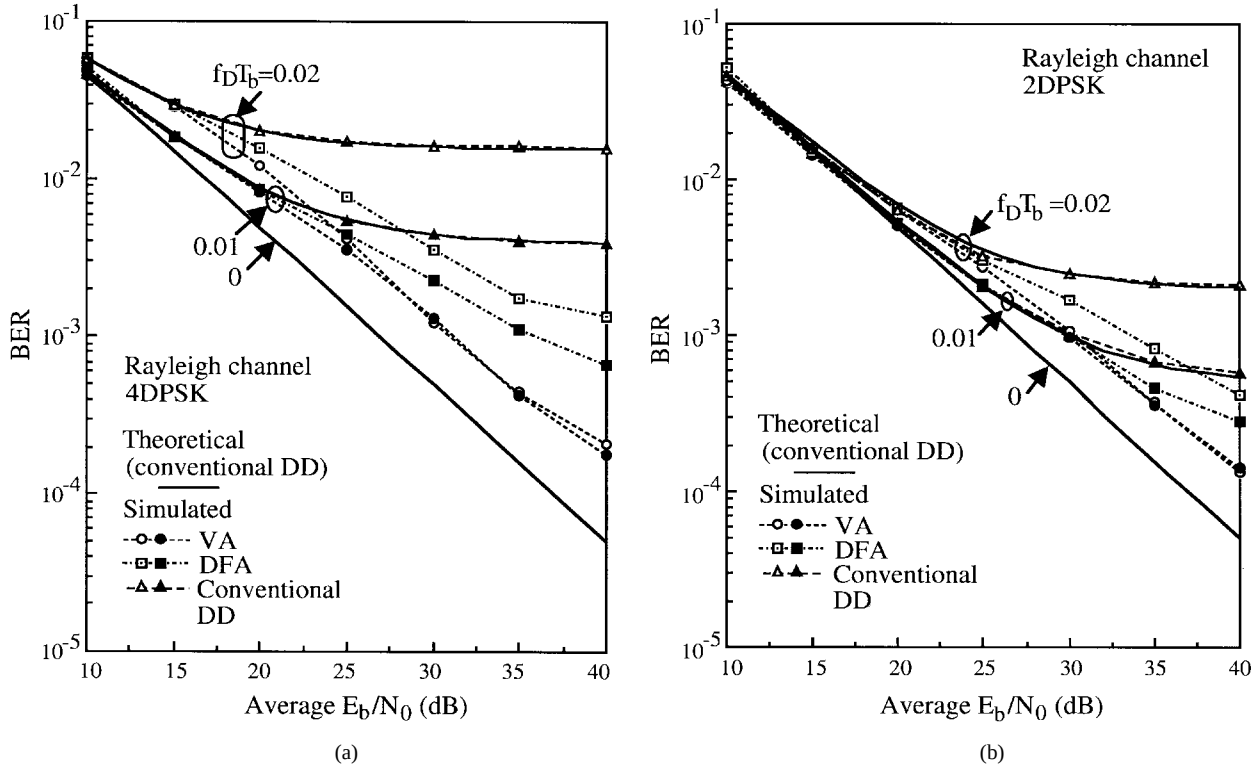

Fig. 7. BER performance in Rayleigh channels: (a) 4DPSK and (b) 2DPSK.

conventional DD, and the following expressions are obtained:

$$\begin{cases} P_{b,\,\mathrm{DFA}} \approx \dfrac{a(M)}{\log_2 M} \dfrac{(\pi f_D T)^4}{\sin^2\left(\dfrac{\pi}{M}\right)} \\ P_{b,\,\mathrm{conventional\,DD}} \approx \dfrac{1}{2} \dfrac{a(M)}{\log_2 M} \dfrac{(\pi f_D T)^2}{\sin^2\left(\dfrac{\pi}{M}\right)}. \end{cases} \tag{46}$$

We observe that adaptive DD can significantly reduce the irreducible BER due to Doppler spread for small f_DT values. The BER's due to Doppler spread calculated from (42) and (44) are plotted in Fig. 6 as solid lines for $M = 2$ and 4.

IV. Computer Simulations

The BER performance of adaptive DD is evaluated by computer simulations for 2 and 4DPSK transmission in AWGN and Rayleigh channels. A Rayleigh-faded signal was generated based on Jakes model [1] assuming constant amplitude, 16 multipaths.

The proposed adaptive DD can adapt the reference signal to changing channel conditions. Fig. 3 shows how quickly the predictor coefficient converges in the case of 4DPSK—the VA was assumed. Predictor coefficient adaptation used $\beta = 1$. The initial value of the predictor coefficient was set to $\hat{\mu}_0 = 0$ (the detection of the first symbol is equivalent to the conventional DD). It was found by simulation that the predictor coefficient converges to $\hat{\mu}_\infty = -0.5$ for AWGN channels with $E_b/N_0 = 7$ dB and $\hat{\mu}_\infty = +0.902$ for Rayleigh channels with average signal energy per bit-to-AWGN power spectrum density ratio $E_b/N_0\ [= (E_s/N_0)/\log_2 M] = 60$ dB and $f_DT_b\ (= f_DT/\log_2 M) = 0.04$. These values are almost the same as expected from Section II-E. The acquisition time defined here is the time required for the predictor coefficient to converge to 90% of the value of $\hat{\mu}_\infty$. It is found from Fig. 3 that the acquisition time is 15 symbols for AWGN channels and 46 symbols for Rayleigh channels. It should be pointed out that even during the acquisition period, the BER performance can be improved over conventional DD since it compensates the effects of AWGN and Doppler spread to some extent.

Fig. 4 shows the effect of the adaptation forgetting factor β on the BER for 4DPSK. For error rate measurements, a number of data frames, each consisting of 2048 symbols, was transmitted. It is seen that the optimum is $\beta = 1$ for AWGN channels [Fig. 4(a)] and that the BER using DFA is sensitive to β. When most errors are produced by Doppler spread, the optimum is $\beta = 0.3$ (0.55) for VA (DFA) at average $E_b/N_0 = 60$ dB [Fig. 4(b)], however, a broad optimum is observed. The same tendency was observed for 2DPSK. Fig. 5 plots the effect of decoding depth D for VA in AWGN channels. The performance is almost insensitive to $D \geq 2$ and in the following simulation, we used $D = 2$.

The irreducible BER due to Doppler spread is plotted in Fig. 6 as a function of f_DT_b for 2 and 4DPSK. As was expected, adaptive DD significantly reduces the irreducible BER. When $f_DT_b = 0.01$, the irreducible BER of conventional DD becomes 3.9×10^{-3} for 4DPSK. Adaptive DD-DFA ($\beta = 0.55$) can reduce it by more than two orders of magnitude, and the use of VA ($\beta = 0.3$) can further reduce it below 10^{-5}. For comparison, the theoretical performances calculated from (42) and (44) are plotted as solid lines for adaptive DD-DFA and conventional DD. The irreducible BER of adaptive DD-DFA increases in proportion to the fourth power of f_DT_b

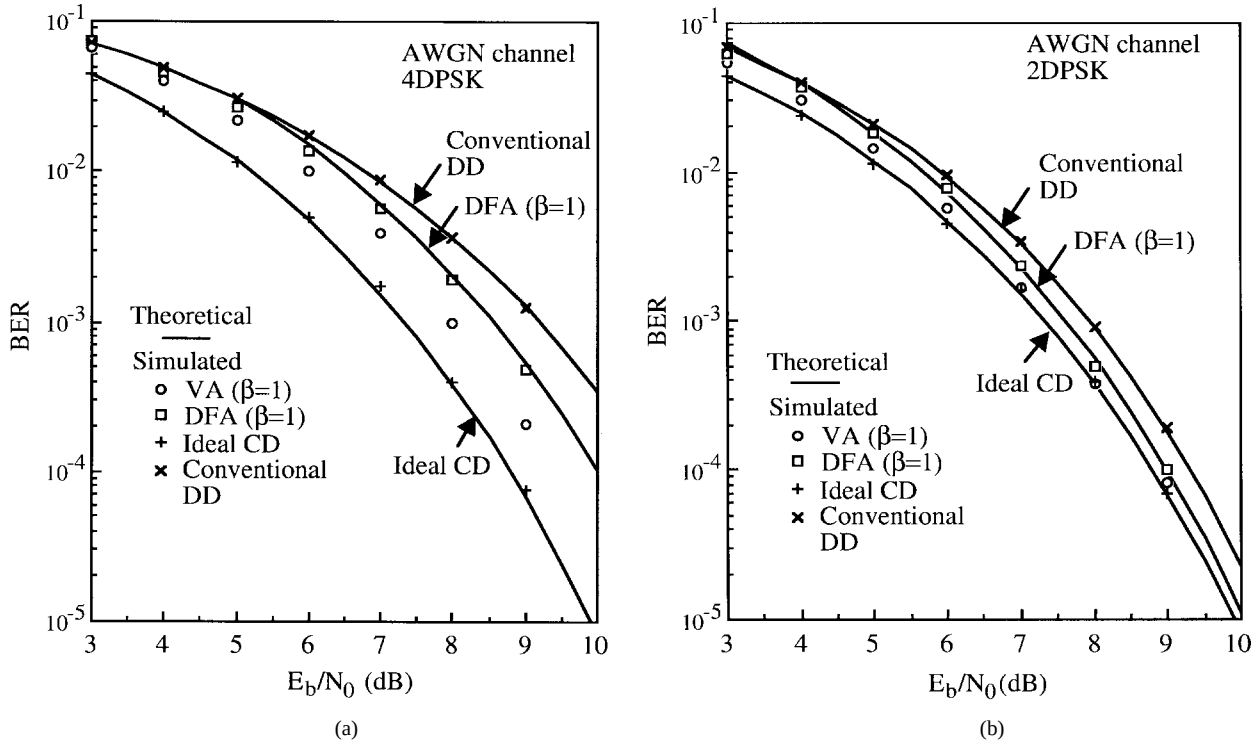

Fig. 8. BER performance in AWGN channels: (a) 4DPSK and (b) 2DPSK.

while that of conventional DD is in proportion to the second power of $f_D T_b$ as (46) indicates. A good agreement between theory and simulation results is obtained. The irreducible BER when $\beta = 1$ is larger than that gained when using the optimum β. However, it is sufficiently reduced compared to that of conventional DD. The irreducible BER of 4DPSK when $f_D T_b = 0.01$ can be reduced to 7.2×10^{-5} (3.9×10^{-4}) for VA (DFA), while 3.9×10^{-3} for conventional DD. Hence, for mobile radio, where a channel can change from an AWGN channel to a Rayleigh channel and vice versa, we can use $\beta = 1$ to effectively adapt to changing channel conditions and achieve an overall gain in performance over conventional DD.

Fig. 7 shows the BER performance using $\beta = 1$ as a function of average E_b/N_0 in Rayleigh fading. Even in the E_b/N_0 regions where errors are produced by the combined effects of AWGN and Doppler spread, adaptive DD performs satisfactorily. When $f_D T_b = 0.02$, the effect of Doppler spread is significantly compensated; the use of VA makes the BER performance close to that in the slow fading case ($f_D T_b \to 0$) with a degradation of only about 5 (4) dB. $f_D T_b = 0.02$ corresponds to the high terminal traveling speed of 173 km/h for 16 kbps and 2-GHz carrier frequency. For comparison, the theoretical BER performance of conventional DD calculated from (44) is plotted as solid lines.

Fig. 8 shows the BER performance ($\beta = 1$) in the AWGN channel. The proposed adaptive DD is also effective in AWGN channels—for the case of 4DPSK, a performance gain of 1.2 (0.7) dB is achieved over conventional DD for VA (DFA) at BER $= 10^{-3}$; the performance becomes close to that of CD with a loss of 0.65 (1.15) dB for VA (DFA). For the case of 2DPSK, the VA provides almost identical performance with CD in small BER regions. For comparison, the theoretical BER performances of adaptive DD-DFA, conventional DD, and CD are plotted in Fig. 8 as solid lines. It can be seen that the simulation results are in good agreement with the theory.

V. Conclusion

An adaptive DD scheme that can reduce significantly the irreducible BER due to Doppler spread was proposed for the reception of M-ary DPSK. It uses the adaptive linear prediction of reference signals based on the RLS algorithm and the phase sequence estimation based on VA and DFA. Theoretical analysis and computer simulations have proved that the irreducible BER due to Doppler spread can be significantly reduced. Furthermore, it was shown that in the AWGN channel, the proposed detection scheme reduces to a multiple symbol DD [4]–[6] using $L = 2$ signal samples. Since the proposed scheme can adapt the reference signal prediction to changing channel conditions, its applications include mobile radio where channels may change from AWGN channels to Rayleigh channels and vice versa according to mobile terminal movement.

Appendix

Using the following formula [11, eqs. (A-3-2) and (A-3-4)]:

$$\begin{cases} 1 + Q(a, b) - Q(b, a) \\ \quad = \dfrac{b^2 - a^2}{b^2 + a^2} \displaystyle\int_{(b^2+a^2)/2}^{\infty} e^{-t} I_0\left(\frac{2ab}{b^2 + a^2}\, t\right) dt \\ \quad b > a > 0 \\ 1 + Q(a, b) - Q(b, a) \\ \quad \approx \operatorname{erfc}\left(\dfrac{b - a}{\sqrt{2}}\right), \qquad b \gg b - a > 0 \text{ and } a,\ b \gg 1 \end{cases} \tag{A1}$$

where $I_0(.)$ is the zeroth-order modified Bessel function and $\mathrm{erfc}(.)$ is the complementary error function, and we have

$$\frac{b^2-a^2}{b^2+a^2}\int_{(b^2+a^2)/2}^{\infty} e^{-t} I_0\left(\frac{2ab}{b^2+a^2}\,t\right) dt \approx \mathrm{erfc}\left(\frac{b-a}{\sqrt{2}}\right). \tag{A2}$$

Substituting the integral representation of the I_0 function

$$I_0(x) = \frac{1}{\pi}\int_0^{\pi} \exp[x\cos\theta]\, d\theta \tag{A3}$$

into (A2) and performing integration with respect to t, we obtain

$$\frac{b^2-a^2}{b^2+a^2}\,\frac{1}{\pi}\int_0^{\pi} \frac{\exp\left[-\dfrac{b^2+a^2}{2}\left(1-\dfrac{2ab}{b^2+a^2}\cos\theta\right)\right]}{1-\dfrac{2ab}{b^2+a^2}\cos\theta}\, d\theta \approx \mathrm{erfc}\left(\frac{b-a}{\sqrt{2}}\right). \tag{A4}$$

Finally, letting $k = 2ab/(a^2+b^2)$ and $x = (a^2+b^2)/2$, we have

$$\frac{1}{\pi}\int_0^{\pi} \frac{e^{-x(1-k\cos\theta)}}{1-k\cos\theta}\, d\theta \approx \frac{1}{\sqrt{1-k^2}}\,\mathrm{erfc}\sqrt{x(1-k)}. \tag{A5}$$

REFERENCES

[1] W. C. Jakes, Jr., Ed., *Microwave Mobile Communications.* New York: Wiley, 1974.

[2] F. Adachi and K. Ohno, "BER performance of QDPSK with postdetection diversity reception in mobile radio channels," *IEEE Trans. Veh. Technol.*, vol. 40, pp. 237–249, Feb. 1991.

[3] S. Haykin, *Adaptive Filter Theory*. Englewood Cliffs, NJ: Prentice-Hall, 1991.

[4] D. Makrakis and K. Feher, "Optimal noncoherent detection of PSK signals," *Electron. Lett.*, vol. 26, pp. 398–400, Mar. 1990.

[5] F. Edbauer, "Bit error rate of binary and quaternary DPSK signals with multiple differential feedback detection," *IEEE Trans. Commun.*, vol. 40, pp. 457–460, Mar. 1992.

[6] F. Adachi and M. Sawahashi, "Decision feedback multiple-symbol differential detection for M-ary DPSK," *Electron. Lett.*, vol. 29, pp. 1385–1387, July 1993.

[7] R. F. Pawula, S. O. Rice, and J. H. Roberts, "Distribution of the phase angle between two vectors perturbed by Gaussian noise," *IEEE Trans. Commun.*, vol. COM-30, pp. 1828–1841, Aug. 1982.

[8] W. C. Lindsey and M. K. Simon, *Telecommunication Systems Engineering.* Englewood Cliffs, NJ: Prentice-Hall, 1979.

[9] F. Adachi and T. T. Tjhung, "Distribution of phase angle between two Rayleigh vectors perturbed by Gaussian noise," *Electron. Lett.*, vol. 28, pp. 923–925, May 1992.

[10] P. J. Lee, "Computation of the bit error rate of coherent M-ary PSK with Gray code bit mapping," *IEEE Trans. Commun.*, vol. COM-34, pp. 488–491, May 1986.

[11] M. Schwartz, W. R. Bennett, and S. Stein, *Communication Systems and Techniques.* New York: McGraw-Hill, 1966.

Fumiyuki Adachi (M'79–SM'90) received the Dr.Eng. degree from Tohoku University, Sendai, Japan, in 1984.

In 1973, he joined Nippon Telegraph and Telephone Corporation (NTT) Laboratories, Japan. In 1992, he transferred to NTT Mobile Communications Network, Inc. At NTT, he worked on the development of a TDMA digital cellular base-station transceiver. Presently, he is a Senior Executive Research Engineer at NTT Mobile Communications Network, Inc., Kanagawa-ken, Japan, where he has been leading a research group for wideband DS-CDMA cellular radio. His research interests also include bandwidth-efficient modulation/demodulation, diversity reception, and channel coding. From 1984 to 1985, he was a United Kingdom SERC Visiting Research Fellow in the Department of Electrical Engineering and Electronics, Liverpool University, Liverpool, U.K. He has written chapters of three books: *Fundamentals of Mobile Communications*, *Mobile Communications*, and *Digital Mobile Communications*.

Dr. Adachi was a corecipient of the IEEE Vehicular Technology Society Paper of the Year Award in 1980 and 1990. He was Secretary of the IEEE Vehicular Technology Society Tokyo Chapter from 1991 to 1994.